

**Growth of correlations in gravitational  $N$ -body simulations**

Thierry Baertschiger\*

*Département de Physique Théorique, Université de Genève, Quai E. Ansermet 24, CH-1211 Genève, Switzerland*

Francesco Sylos Labini†

*Laboratoire de Physique Théorique, Université Paris XI, Bâtiment 211, F-91405 Orsay, France*

(Received 13 January 2004; published 1 June 2004)

In the gravitational evolution of a cold infinite particle distribution, two-body interactions can be predominant at early times: we show that, by treating the simple case of a Poisson particle distribution in a static universe as an ensemble of isolated two-body systems, one may capture the origin of the first nonlinear correlated structures. The developed power-law-like behavior of the two-point correlation function is then simply related to the functional form of the time-evolved nearest-neighbor probability distribution, whose time dependence can be computed by using the Liouville theorem for the gravitational two-body problem. We then show that a similar dynamical evolution is also found in a large-scale ordered distribution, which has striking similarities to the case of a cosmological cold dark matter simulation which we also consider.

DOI: 10.1103/PhysRevD.69.123001

PACS number(s): 95.10.Ce, 05.45.-a, 45.05.+x, 98.65.-r

**I. INTRODUCTION**

Nonlinear gravitational clustering can be studied by means of  $N$ -body simulations (NBS) which compute numerically the evolution of a system of particles under the action of their mutual gravity. The gravitational many-body problem consists in the explanation of the time evolution of the NBS and in the theoretical understanding of the formation of nonlinear structures. Up to now, two different approaches have been generally studied: the first involves research of approximate solutions of the Bogoliubov-Born-Green-Kirwood-Yvon (BBGKY) hierarchy [1], and the second explores statistical thermodynamics mainly developed by Saslaw [2].

A main issue in the context of cosmological NBS is to relate the formation of nonlinear structures to the specific choice of initial conditions used: this is done in order to constraint models with observations of cosmic microwave background radiation anisotropies, which are related to the initial conditions, and of galaxy structures, which give instead the final configuration of strongly clustered matter. Standard primordial cosmological theoretical density fields, such as the cold dark matter (CDM) case, are Gaussian and made of a huge number of microscopic mass particles, which are usually treated theoretically as a self-gravitating collisionless fluid [3–5]: this means that the fluid must be dissipationless and that two-body scattering should be small. The problem is then in which limit NBS, based on particle dynamics, are able to reproduce the above two conditions. In this context, one has to consider the issue of the physical role of particle fluctuations in the dynamics of NBS as the total energy is conserved during time evolution (the only mechanism of energy dissipation is related to local gravitational processes).

In fact, in the discretization of a continuous density field one faces two important limitations corresponding to the new

length scales which are introduced. On the one hand, a relatively small number of particles are used: this introduces a mass scale which is the mass of these particles. (In typical cosmological NBS, this mass is of the order of a galaxy and hence many orders of magnitude larger than the microscopic mass of a CDM particle.) Furthermore, it introduces a new characteristic length scale given by the average distance between nearest-neighbor (NN) particles  $\langle \Lambda \rangle$ . Clearly the discretization method used should conserve the continuous correlations, but this is a problematic aspect of standard methods [6–10]. On the other hand, one must smooth the gravitational force at small scales in order to avoid problems related to the divergence of the numerical integrator and remove collisional effects due to strong scattering between particles. This is usually done by using a softening length  $\epsilon$  in the gravitational potential generally defined as

$$\phi(r) = -\frac{1}{\sqrt{\epsilon^2 + r^2}}. \quad (1)$$

This is the second length scale introduced to numerically simulate the collisionless fluid.

The question which naturally arises is then how to choose the two new length scales  $\langle \Lambda \rangle$  and  $\epsilon$ : the first obvious condition is that they must both be smaller than the intrinsic characteristic scales of the continuous field (that is, smaller than the typical scale corresponding to the turnover scale of the CDM power spectrum). Then one has to tune the ratio  $\eta = \langle \Lambda \rangle / \epsilon$  appropriately with respect to the physical problem under study. In fact, when  $\eta > 1$  one has a larger dynamical range than the case  $\eta < 1$ , but strong scattering between nearby particles is not smoothed and hence one is not effectively reproducing a dynamics where particles play the role of collisionless fluid elements. It is in this sense that one talks about the role of discreteness in NBS, namely that strong scattering between nearby particles is produced by the discretization and by the choice of  $\eta > 1$ , and it should be considered artificial and spurious with respect to the dynamical evolution of a self-gravitating fluid. This point has been

\*Electronic address: Thierry.Baertschiger@physics.unige.ch

†Electronic address: Francesco.Sylos-Labini@th.u-psud.fr

considered in different ways and contexts by many authors, e.g., [3–5,11–14]: they all show that discreteness has some influence on the formation of the structures.

For this reason, discreteness, which nevertheless introduces large fluctuations in the density field up to scales of order  $\langle \Lambda \rangle$ , may play an important role in the early stages of nonlinear structure formation, i.e., when the average distance between nearby particles becomes rapidly smaller than  $\langle \Lambda \rangle$ . How discrete effects are then “exported” toward large scales, if they are at all, is a complex and difficult problem to understand. In other words, the problem is that of understanding whether large nonlinear structures, which at late times contain many particles, are produced solely by the collisionless dynamics of a fluid and its density fluctuations or whether the particle collisional processes are important also in the long term. For example, in [11] it was argued that discreteness effects play an important role in the self-similar evolution of correlated structures, while the effect of NN interactions has been the subject of a toy model developed in [12].

In [15,16] we have already considered the effects of discretization in the dynamics of nonlinear structure formation in several NBS with and without space expansion. We have concluded that the fluctuations at the smallest scales in these NBS—i.e., those associated with the discreteness of the particles—play a central role in the dynamics of clustering in the nonlinear regime. This was based, in particular, on the fact that the correlations appear to be built up from the initial clustering at the smallest scales and that the nature of the clustering seems to be independent of (or at most very weakly dependent on) the initial conditions. The theoretical understanding of the creation of these correlations should therefore deal with the apparently crucial role of the intrinsically highly fluctuating initial density field.

In this paper, we put our previous results on a firmer physical basis. We study the formation of first structures in several NBS. As a reference example, we use a cold (zero initial velocity) Poisson distribution as initial conditions and we consider the case of a nonexpanding background, i.e., a static universe. In this case, we show that two-body interactions are enough to explain the evolution of the correlation function at early times, as has been already noticed in [17]. This is done by treating the  $N$ -body problem as an ensemble of isolated two-body systems. Such an approximation is justified, in the Poisson case, by the fact that the probability that nearby particles are mutually NN is high enough ( $\sim 0.6$ ) (becoming of order 1 when very close particles are only considered) and by the fact that the NN force is the dominating one [18]. Using the Liouville theorem for the gravitational two-body problem, we can find the early evolution of the NN probability distribution. As this distribution can be linked to the conditional density and therefore to the reduced two-point correlation function, we also obtain their evolution at early times. Comparing with the results from the simulations, we find excellent agreement: this shows that the first structures observed are a consequence of two-body interactions between NNs. After a time of the order of the typical time scale of two-body interaction, this is of course not the case anymore. However, we note that the functional behavior of

the two-point correlation function remains unchanged at later times, while the regime of strong clustering increases with time.

We then study in the same perspective three other different simulations in which the force is not dominated by short-scale contributions since the beginning. The link between the NN probability distribution is found to be an efficient tool to study the nature of the first correlations developed and the growth of power-law correlations when high-resolution ( $\eta \gg 1$ ) NBS are considered.

## II. STATISTICAL TOOLS

A simple tool used to study clustering of a matter distribution is the *two-point correlation function* [19]  $\langle n(\mathbf{r}_1)n(\mathbf{r}_2) \rangle$ , which gives the probability density for finding one particle around  $\mathbf{r}_1$  and a second one around  $\mathbf{r}_2$  [ $n(\mathbf{r})$  being the microscopic mass density function]. In the following, we will restrict ourselves to distributions which have a well-defined average density  $n_0$  and are homogeneous and isotropic. In that case, the two-point correlation function only depends on  $r_{12} = |\mathbf{r}_1 - \mathbf{r}_2|$  and the asymptotic average density is positive. This function is useful to study both continuous and discrete distributions of matter. In the latter case, which is the case of interest here, it can be useful to measure averages from a point occupied by a particle. For instance, one can define the *conditional density*

$$\langle n(r) \rangle_p \equiv \frac{\langle n(\mathbf{0})n(\mathbf{r}) \rangle}{n_0} \quad (2)$$

for  $r > 0$ ; this gives the average density at a distance  $r$  from an occupied point.<sup>1</sup> It is easy to show that one has the following relation:

$$\langle n(r) \rangle_p \equiv n_0 [1 + \xi(r)] \quad \text{for } r > 0, \quad (3)$$

where  $\xi(r)$  is the *nondiagonal part of the reduced two-point correlation function* [19].

In order to study small-scale properties of a discrete distribution, one may consider the *nearest-neighbor probability distribution*  $\omega(r)$ . This gives the probability density of the distance from a particle to its NN [18]. Let us briefly discuss its relation to the average conditional density. By definition, the probability that, given a particle, there is another particle in the infinitesimal volume element  $dV$  at distance  $r$  is

$$p_1(r) = \langle n(r) \rangle_p dV. \quad (4)$$

Now we only have to note that the probability  $\omega(r)dr$  for a given particle having a NN at a distance between  $r$  and  $r + dr$  is the probability of having no NN in the sphere of radius  $r$  centered on the particle multiplied by the probability of having one particle in the infinitesimal spherical shell around this sphere,

<sup>1</sup> $\langle \rangle_p$  means that it is a conditional average: the origin is an occupied point.

$$\omega(r)dr = \left(1 - \int_0^r \omega(s)ds\right) \langle n(r) \rangle_p 4\pi r^2 dr, \quad (5)$$

where the second part of the right-hand side is the probability  $p_1(r)$  with  $dV = 4\pi r^2 dr$ .

### III. EVOLUTION OF A POISSON DISTRIBUTION

In the case of a Poisson distribution, one simply has  $\langle n(r) \rangle_p = n_0$  [19]. It is then easy to solve Eq. (5) for  $\omega(r)$ . One finds [18]

$$\omega(r) = 4\pi n_0 r^2 \exp\left(-\frac{4}{3}\pi n_0 r^3\right). \quad (6)$$

The average distance between a particle and its NN is given by

$$\langle \Lambda \rangle = \int_0^\infty r \omega(r) dr = \left(\frac{3}{4\pi n_0}\right)^{1/3} \Gamma_E\left(\frac{4}{3}\right), \quad (7)$$

where  $\Gamma_E$  is the Euler incomplete gamma function.

Let us now compute the probability, in a Poisson distribution, that given a particle and its NN, they are mutually NN. Let us suppose that a particle  $A$  has the particle  $B$  as its NN at distance  $r$ . The probability that  $A$  is the NN of  $B$  is equal to the probability that no other particles are in the volume  $v(r)$  defined by the portion of the sphere of radius  $r$  around  $B$  which is not contained in the sphere of radius  $r$  around  $A$ . For a Poisson distribution this is simply<sup>2</sup>

$$p_2(r) = \exp(-n_0 v(r)), \quad (8)$$

where  $v(r)$  is given by

$$v(r) = \frac{11}{12}\pi r^3. \quad (9)$$

Averaging on  $r$ , we get the probability that two particles are mutually NN,

$$p_3 = \int_0^\infty \omega(r) \exp(-n_0 v(r)) dr \approx 0.6. \quad (10)$$

Hence we have that more than half of the particles are mutually NN. If we restrict ourselves to particles which have a NN at a distance  $l < \langle \Lambda \rangle$ , this probability becomes

$$p_4 = \frac{\int_0^{\langle \Lambda \rangle} \omega(r) \exp(-n_0 v(r)) dr}{\int_0^{\langle \Lambda \rangle} \omega(s) ds} \approx 0.8. \quad (11)$$

This result, together with the fact that in a Poisson distribution the force on a particle is mainly due to its NN [18],

allows us to consistently treat for an initial short time the many-body problem as an ensemble of independent and isolated two-body systems.

#### A. Time scale of NN interaction

This last result explains what happens if one leaves a Poisson distribution without velocity evolving under its own gravity: most of particles will fall on their NN. Let us determine the time scale of this phenomenon. To this aim, one can use conservation of energy in a pair of particles of mass  $m$ ,

$$E = -\frac{Gm^2}{r_0} = \frac{m}{2}(\dot{\mathbf{x}}_1^2 + \dot{\mathbf{x}}_2^2) - \frac{Gm^2}{r(t)}, \quad (12)$$

where we have used the Newtonian potential. As we will see in more detail in the next subsection, the problem can be reduced to a single dimension, and choosing center-of-mass coordinates we get  $x_1(t) = -x_2(t)$ . After some algebraic manipulations, Eq. (12) becomes

$$\dot{x}_1 = -\sqrt{Gm\left(\frac{1}{2x_1} - \frac{1}{r_0}\right)} \quad (13)$$

assuming that  $x_1(0) > 0$ . The time of fall is

$$t_{\text{fall}}(r_0) = -\int_{r_0/2}^0 \left[Gm\left(\frac{1}{2x} - \frac{1}{r_0}\right)\right]^{-1/2} dx \\ = \frac{r_0^{3/2} \pi}{4} \frac{1}{\sqrt{Gm}}. \quad (14)$$

Taking for  $r_0$  the mean distance between NNs,  $\langle \Lambda \rangle$  given by Eq. (7), we get

$$\tau = \frac{\pi}{4} \sqrt{3\Gamma_E^3(4/3)} \frac{1}{\sqrt{4\pi G \rho_0}} \approx \frac{1.148}{\sqrt{4\pi G \rho_0}}, \quad (15)$$

where  $\rho_0 = mn_0$  is the mass density.

#### B. Approximate evolution of the conditional average density

As already mentioned, the force on a particle in a Poisson distribution is almost only due to its NN. As in our simulations, the particles have no initial velocity. They will start to fall in the direction of their NN, and we will see that this is what explains the early evolution of  $\langle n(\mathbf{r}) \rangle_p$  for a time  $t \lesssim \tau$ .

Let us consider that the interaction potential is  $U(\mathbf{r}) = U(r)$ .<sup>3</sup> As we said before, we make the assumption that the force on a particle is only due to its NN and that the Poisson distribution can be approximated by an ensemble of particle pairs evolving independently. The evolution of one of these pairs is given by the following equations:

<sup>2</sup>In a Poisson distribution, the probability that there are  $k$  particles in a volume  $V$  is given by  $(n_0 V)^k \exp(-n_0 V)/k!$ .

<sup>3</sup>We do not restrict ourselves to a precise potential as it can vary in different NBS.

$$m\ddot{\mathbf{x}}_1 = -\nabla_{\mathbf{x}_1} U(r_{12}) = -\frac{dU}{dr}\bigg|_{r_{12}} \cdot \frac{\mathbf{x}_1 - \mathbf{x}_2}{r_{12}}, \quad (16a)$$

$$m\ddot{\mathbf{x}}_2 = -\nabla_{\mathbf{x}_2} U(r_{12}) = +\frac{dU}{dr}\bigg|_{r_{12}} \cdot \frac{\mathbf{x}_1 - \mathbf{x}_2}{r_{12}}, \quad (16b)$$

with  $r_{12} = |\mathbf{x}_1 - \mathbf{x}_2|$ . Adding these two equations, one gets  $\ddot{\mathbf{x}}_1 = -\ddot{\mathbf{x}}_2$  (conservation of total momentum). As the particles are supposed to be at rest at  $t=0$ , one has  $\mathbf{x}_1 = -\mathbf{x}_2$  with a proper choice of the origin (center-of-mass coordinates). With this relation,  $\mathbf{x}_1 - \mathbf{x}_2 = 2\mathbf{x}_1 = -2\mathbf{x}_2$  and one has to solve only one equation of motion, for instance for particle 1,

$$m\ddot{\mathbf{x}}_1 = -\frac{dU}{dr}\bigg|_{2|\mathbf{x}_1|} \cdot \frac{\mathbf{x}_1}{|\mathbf{x}_1|}. \quad (17)$$

Using again the fact that the initial velocity is null, one can reduce the number of dimensions to one,

$$m\ddot{x} = -\frac{dU}{dr}\bigg|_{2|x|} \cdot \text{sgn}(x) = -\frac{dV}{dx} \quad (18)$$

with  $V(x) = U(|2x|)/2$ , which is the equation for the evolution of a single particle in the potential  $V$ . One can now use the Liouville theorem [20] in order to study the evolution of a phase-space density function of systems evolving according to this equation, and by choosing an appropriate density function one can obtain the evolution of  $\omega(r)$ .

If  $f(x, v, t)$  is a phase-space density function, the Liouville theorem states that

$$(\partial_t + v\partial_x + \dot{v}\partial_v)f = 0, \quad (19)$$

where, in our case,  $m\dot{v} = -dV/dx$ . The appropriate initial condition is

$$f(x, v, 0) = \delta(v) \frac{\omega(2|x|)}{2}, \quad (20)$$

with  $\omega(r)$  given by Eq. (6). We divide it by 2 in order to have half of the particles with  $x > 0$  and half with  $x < 0$ . Knowing  $f(x, v, t)$ , one can obtain  $\omega(r, t)$ , the time-evolved NN probability distribution, with

$$\begin{aligned} \omega(r, t) &= \int_{-\infty}^{\infty} f(-r/2, v, t) dv \\ &+ \int_{-\infty}^{\infty} f(r/2, v, t) dv. \end{aligned} \quad (21)$$

In order to solve the Liouville equation, let us denote by  $\phi_t(x_0, v_0) = (X_t(x_0, v_0), V_t(x_0, v_0))$  the solution of the equation of motion with initial condition  $x_0, v_0$  at  $t=0$ . The Liouville equation implies that  $f(x, v, t)$  remains constant along a phase-space trajectory,

$$f(X_t(x_0, v_0), V_t(x_0, v_0), t) = f(x_0, v_0, 0). \quad (22)$$

With our initial conditions, the solution of this equation is therefore

$$\begin{aligned} f(x, v, t) &= f(\phi_{-t}(x, v), 0) \\ &= \int \int_{\mathbb{R}^2} dx_1 dv_1 [f(\phi_{-t}(x_1, v_1), 0) \\ &\quad \times \delta(x - x_1) \delta(v - v_1)] \\ &= \int \int_{\mathbb{R}^2} dx_0 dv_0 [f(x_0, v_0, 0) \\ &\quad \times \delta(x - X_t(x_0, v_0)) \delta(v - V_t(x_0, v_0))] \end{aligned} \quad (23)$$

with  $f(X_t(x, v), V_t(x, v), t) \equiv f(\phi_t(x, v), t)$ . We have used the fact that the determinant of the Jacobian matrix in the change of variables from  $(x_1, v_1)$  to  $(x_0, v_0)$  is  $\det(\partial\phi_t/\partial(x, v)) = 1$ . This is actually related to the Liouville theorem [21].

With this solution, we can get the evolution of  $\omega(r, t)$ . First let us remark that  $f(x, v, 0) = f(-x, -v, 0)$ , and as the force in Eq. (18) is odd, if  $x(t)$  is a solution,  $-x(t)$  is also a solution. This enables us to show that  $f(x, v, t) = f(-x, -v, t)$ . It is then easy to see that Eq. (21) can be rewritten as

$$\omega(r, t) = 2 \int_{-\infty}^{\infty} f(r/2, v, t) dv. \quad (24)$$

Using this last equation and Eq. (23), one has

$$\begin{aligned} \omega(r, t) &= 2 \int_{-\infty}^{\infty} dx_0 \int_{-\infty}^{\infty} dv_0 f(x_0, v_0, 0) \\ &\quad \times \delta(r/2 - X_t(x_0, v_0)). \end{aligned} \quad (25)$$

As  $f(x, v, 0) = \delta(v) \omega(2|x|)/2$ , this becomes

$$\omega(r, t) = \int_{-\infty}^{\infty} dx_0 \omega(2|x_0|) \delta(r/2 - X_t(x_0, 0)). \quad (26)$$

Using the fact that for a function  $f: \mathbb{R} \rightarrow \mathbb{R}$  one has

$$\delta(f(x)) = \sum_{y \in Z(f)} \frac{\delta(x - y)}{|f'(y)|} \quad (27)$$

with  $Z(f) = \{y \in \mathbb{R} | f(y) = 0\}$ , we get

$$\omega(r, t) = \sum_{x_0 \in S_t^r} \left| \frac{dX_t(x_0, 0)}{dx_0} \right|^{-1} \omega(2|x_0|) \quad (28)$$

with  $S_t^r = \{x_0 \in \mathbb{R} | X_t(x_0, 0) = r/2\}$ . Of course there are points  $x_0$  in  $S_t^r$  such that  $dX_t(x_0, 0)/dx_0 = 0$  and therefore  $\omega(r, t)$  is not well defined at some isolated points.

We may solve Eq. (18) numerically to find a solution for  $X_t(x_0, 0)$ . The steps to get  $\omega(r, t)$  for a given  $t$  are the following. We start with a set  $\{x_{0,i} = x_{0,\min} + i\delta | \delta > 0, 0 \leq i \leq n\}$ , where  $x_{\min}$ ,  $\delta$ , and  $n$  are chosen so that the region covered gives non-negligible values for  $\omega(2x)$  and that this region is sufficiently sampled. For each  $i$ , one calculates numerically  $X_i \equiv X_t(x_{0,i}, 0)$ . By doing a linear interpolation with

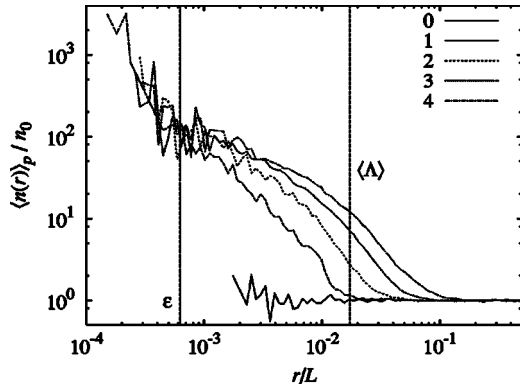


FIG. 1. The normalized conditional density in a Poisson distribution at time  $\tau, 2\tau, 3\tau, 4\tau$ . Note that once correlations are developed, the subsequent evolution increases the range of scales where nonlinear  $[\langle n(r) \rangle_p \gg n_0]$  clustering is formed, while the function behavior of two points remains unchanged.

these values, we have an estimate of  $X_t(x_0, 0)$  for all  $x_0$  in the region covered by the  $x_{0,i}$ . The last step is to find the set of  $x$  which solves  $X_t(x, 0) = r/2$ . Once we have  $\omega(r, t)$ , we find the conditional density by using Eq. (5).

### C. Comparison with a simulation

In order to test the simple argument presented in the preceding subsection, we did an  $N$ -body simulation. We have used the code GADGET [22] based on a tree algorithm. The infinite universe is simulated by using periodic boundary conditions and the usual Ewald summation technique. The force between two particles is not exactly Newtonian but a softened one is used [23]. Note that the potential used is not the standard Plummer one but a similar one which has the advantage of being perfectly Newtonian at a scale larger than the softening length.

We have generated a Poisson distribution with  $N = 32^3$  particles in a box of nominal size  $L$ . The mass of the particles is such that the mass density is 1. The softening length is  $\epsilon = 0.00175L$ : by using Eq. (7) we find  $\langle \Lambda \rangle \approx 0.017L$  and hence  $\eta \approx 10$ . The initial velocities are set to zero, and the simulation is run up to  $4\tau$ .

The time evolution of the conditional density is shown in Fig. 1 [here and in what follows, we normalize the conditional average density to the asymptotic density, i.e., we consider  $\langle n(r) \rangle_p / n_0$ ]. It is worth noticing that once the power-law correlations are developed, the subsequent evolution increases the range of scales where nonlinear clustering is formed, i.e., where  $\langle n(r) \rangle_p \gg n_0$ , by approximately a simple rescaling: denoting by  $\langle n(r, t) \rangle_p$  the conditional density at time  $t$ , one has

$$\langle n(r, t + \delta) \rangle_p \approx \langle n(ar, t) \rangle_p, \quad (29)$$

where  $a > 0$  is a constant which depends on the time [16].

In Fig. 2, we show the initial NN density distribution obtained from the Poisson distribution used in the simulation and the one from Eq. (6). The conditional density of the initial configuration together with the one obtained by using Eq. (5) are shown in Fig. 3.

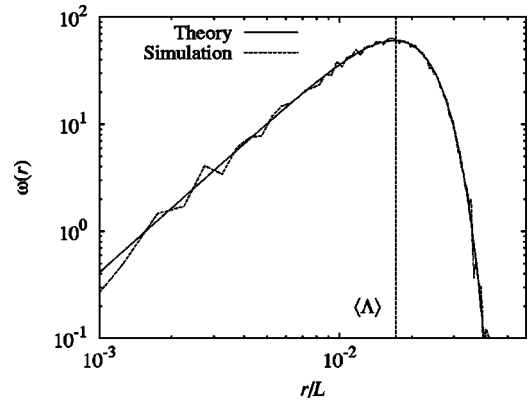


FIG. 2. Initial NN probability distribution for the Poisson case. The solid line is the exact solution given by Eq. (6) while the dashed line is the measured one in the simulation.

The evolution of the NN probability distribution in the simulation together with the one obtained from Eq. (28), at times  $0.5\tau, \tau$ , and  $1.5\tau$ , are shown in Figs. 4–6. We may notice that the agreement is quite good and even excellent at  $t = 0.5\tau$ . The differences which appear at  $t = \tau$  and  $t = 1.5\tau$  seem to be explained by the following arguments.

First of all, we remind the reader that in a Poisson distribution the force acting on a particle can be decomposed in two terms, namely the one given by the NN particle and the one due to all the other particles. While the first represents a large contribution, the second rapidly goes to zero for symmetry reasons [18]. However, for particles which have a NN further than the average  $\langle \Lambda \rangle$ , the situation is different. Let us denote such a particle by  $A$  and its NN by  $B$ . Since the force  $F_{BA}$  from the latter on  $A$  is weaker than the average force on a particle from its NN, the force contribution of other particles nearby also becomes important with regard to the total force on  $A$ . This total force is then not necessarily in the direction of  $B$  and the particle  $A$  will not “fall” on it. Furthermore, the particle  $B$  has a high probability of having a NN different from  $A$ ; it should therefore not go towards  $A$ . The distance between  $A$  and its NN  $B$  should then grow. This

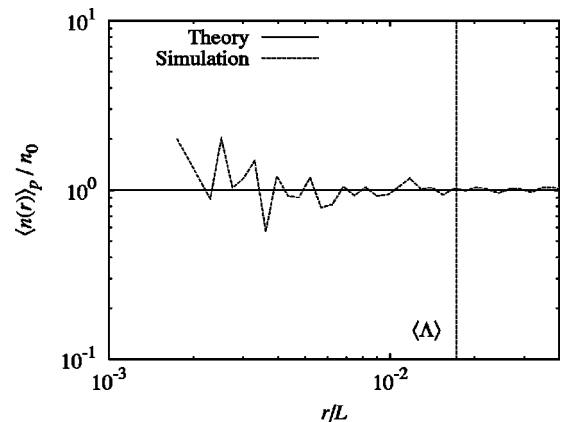


FIG. 3. Normalized two-point conditional density at the initial time: the solid line (theory) is the theoretical ensemble average behavior while the dashed line is the measured one in the simulation.

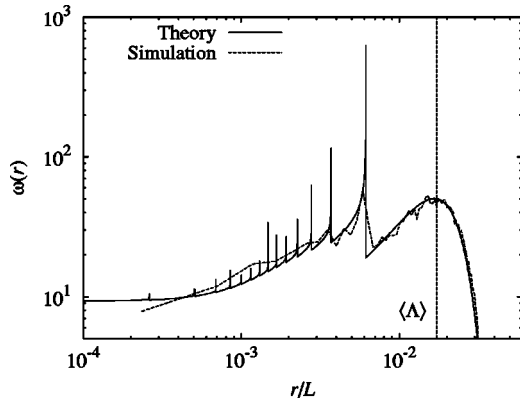


FIG. 4. NN probability distribution at  $t=0.5\tau$  in the Poisson simulation.

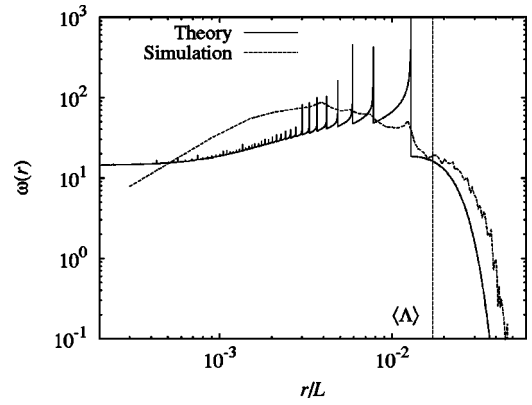


FIG. 6. NN probability distribution at  $t=1.5\tau$  in the Poisson simulation.

is actually what we observe if we compare carefully Figs. 2 and 6: looking at the value of  $r/L$  at large scales at which the NN probability distribution reaches a value of  $10^{-1}$ , we see that it is  $3 \times 10^{-2}$  at  $t=0$  and  $3.5 \times 10^{-2}$  at  $t=1.5\tau$ , i.e., the particles whose NN is at a distance  $3 \times 10^{-2}L$  initially are at a larger distance ( $3.5 \times 10^{-2}L$ ) at  $t=1.5\tau$ .

Secondly, concerning particles which have their NN at a distance closer than the average  $\langle \Lambda \rangle$ , we observe that at scales between  $10^{-3}L$  and  $5 \times 10^{-3}L$  a bump is created: our simple model predicts fewer particles than observed in the simulation. This seems to be a sign of the creation of larger structures. If two particles are isolated, they will move in a regular oscillating motion. This is what the model predicts. In the simulation, these two particles, i.e., a particle and its NN, will move together for a while as in the model, but at the same time they will be attracted toward another pair or group of particles, which is not described by the model. This could have the effect of bringing the two particles closer together and could even give rise to an exchange of NN with the other group of particles, causing the evolution of the NN probability distribution to be different from that in the model. The bump reflects, therefore, this step of the clustering which tends to bring pairs together.

In Figs. 7–9, we compare the predictions of the conditional density given by our model with the measured ones

from the simulations at times  $0.5\tau$ ,  $\tau$ , and  $1.5\tau$ . One sees again that our approximation works really well as it succeeds in reproducing the development of the correlations. This means that these correlations are therefore only a consequence of the interaction of NNs. We may also notice an interesting thing: at  $t=1.5\tau$ , even if the agreement is marginally good at scales larger than  $10^{-3}L$ , it is still correct at smaller scales. An explanation is that these scales correspond to pairs whose particles were very close (i.e.,  $< \langle \Lambda \rangle$ ) initially and were therefore well bounded. When they start to feel the effect of the surrounding particles, their relative motion is not affected and is still described by a two-body interaction.

At larger scales, where there are no correlations, our approximation fails to reproduce the correct behavior at all times. For a certain  $r$  the conditional density goes rapidly to 0. This is due to the fact that at these scales, the NN probability distribution is really small and Eq. (5) is not valid anymore: this equation implies that the density around a particle is only due to its NN and that there are no particles further than the NN. Therefore, at distances larger than the average distance between NNs, the density has to go to 0 as there are no other particles to maintain a nonzero density.

We finally remark that, as noticed in [16], to study the role of these NN interactions in the evolution of clustering, one may modify the force integrator of the numerical code to include *only* the NN contribution to the gravitational force.

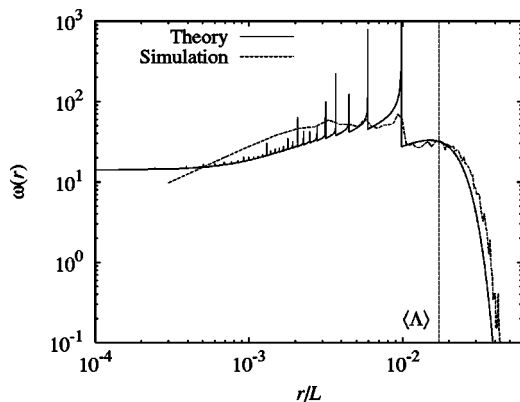


FIG. 5. NN probability distribution at  $t=\tau$  in the Poisson simulation.

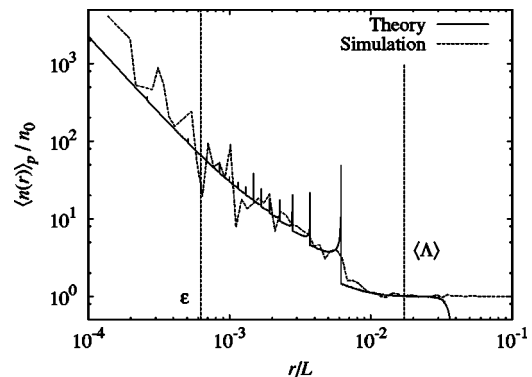


FIG. 7. Behavior of the average conditional density at  $t=0.5\tau$  in the Poisson simulation.

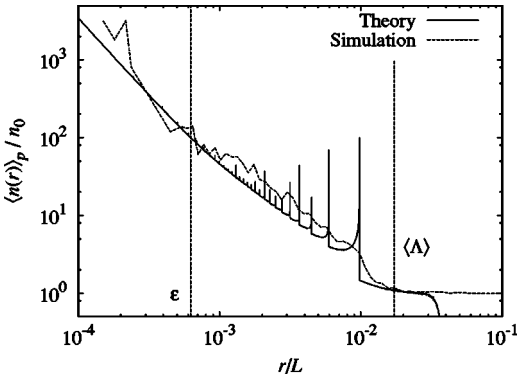


FIG. 8. Behavior of the average conditional density at  $t = \tau$  in the Poisson simulation.

Of course, the result agrees perfectly with the study presented here.

**D. Poisson simulation with large softening**

In the Poisson simulation, we have observed that the first structures created are pairs of particles. Now we present another simulation in which this is not the case. It is simply a Poisson simulation with a large softening, 100 times larger than in the previous case:  $\epsilon = 0.175L$  and hence  $\eta \approx 0.1$ .

Figure 10 shows the evolution of the conditional density in this simulation. The time is still in units of  $\tau$  but only for comparison with the first Poisson simulation, because this is no longer a microscopic characteristic time. One can see that the correlations do not develop at the smallest scales of the system ( $\langle \Lambda \rangle = 0.017L$ ) but are directly found up to  $10^{-1}L$ , which is of the order of  $\epsilon$ .

Looking now at Figs. 11–14, where we compare the conditional densities obtained from the simulation with those reconstructed from the NN probability distributions, we see that as soon as correlations develop, they are already made of many particles as the approximations of the conditional density by the NN probability distribution fail.

In the beginning of this simulation, the NN contribution to the total force acting on a particle is clearly not important. The dominant contribution is actually the force due to many particles at some larger scales. This means that two nearby particles do not fall on each other as in the previous case but

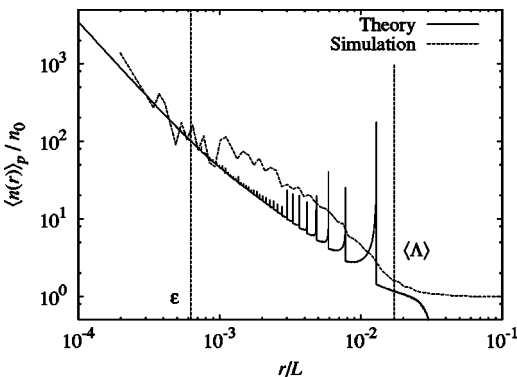


FIG. 9. Behavior of the average conditional density at  $t = 1.5\tau$  in the Poisson simulation.

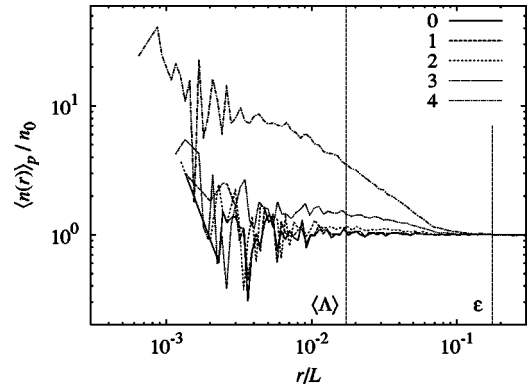


FIG. 10. Evolution of the normalized conditional density in the Poisson simulation with large softening simulation. The times are 0,1,2,3,4 in units of  $\tau$ .

feel approximately the same force and therefore go in the same direction once the simulation starts. This direction should be the one of the nearest mass overdensity. Some other particles will also be attracted in this direction. The effect of this motion is the formation of the first structures, directly made of more than two particles.

As a final remark, it is interesting to note that when power-law correlations are formed at  $t \approx 4\tau$ , the exponent and the amplitude of the conditional density agree very well with the small softening simulation that was previously discussed.

**IV. THE SHUFFLED LATTICE AND THE CDM CASE**

We study now two different cases in which the average force on a particle in the initial distribution is different from the Poisson case, i.e., it is not dominated by the NN one. The main point here is to use the relation (5) to study the creation of the first structures: by obtaining the NN probability distribution in a simulation, we reconstruct the conditional density and compare it with the one measured directly in the simulation.

**A. The shuffled lattice**

A shuffled lattice is a simple ordered distribution [19] which is obtained by adding a random small perturbation to

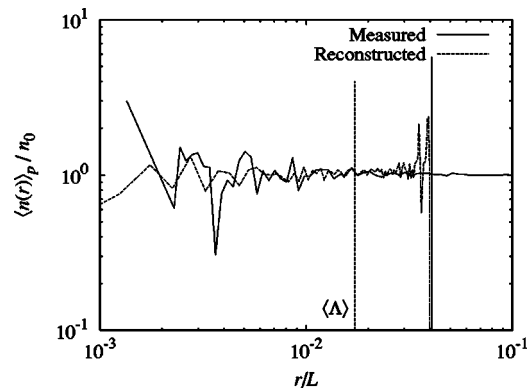


FIG. 11. Reconstruction of the conditional density from  $\omega(r)$  at  $t = 0$  in the Poisson simulation with large softening simulation.

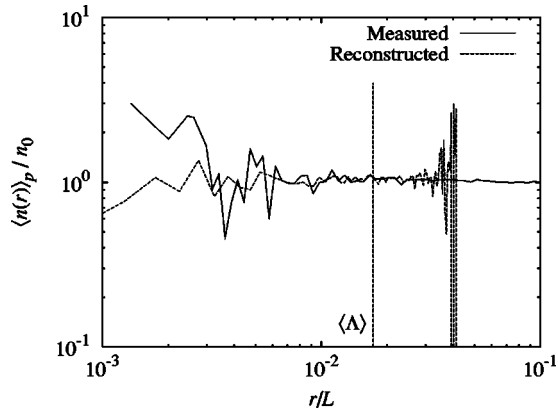


FIG. 12. Reconstruction of the conditional density from  $\omega(r)$  at  $t = \tau$  in the Poisson simulation with large softening simulation.

a perfect lattice of particles: each particle of this lattice is moved randomly in a cubic box centered on the unperturbed position of the particle. The only parameter is then the ratio

$$a_s = \frac{\delta}{l} \quad (30)$$

between the size of the cubic box  $2\delta$  and the lattice spacing  $l$ . When  $a_s=0$  it is a perfect lattice, while as  $a_s \rightarrow \infty$  it becomes a Poisson distribution [19]. For the simulation presented here, we have used a shuffled lattice with  $32^3$  particles and a shuffling parameter  $a_s=0.25$ . The mass of the particles, the number density, and the softening length of the force are the same as for the Poisson simulations previously discussed: this gives  $\eta \approx 14$ .

In Fig. 15, the evolution of the conditional density is shown. The time goes from 0 to  $4\tau$  with  $\tau$  given by Eq. (15). One may note that once correlations are developed, the evolution proceeds in a very similar way to the Poisson case (see Fig. 1): it is the same kind of rescaling as given by Eq. (29), the only difference being the speed at which this happens [16].

In Fig. 16, we show the NN probability distribution measured in the simulation at the corresponding times. It is important to note that at  $t=0$  there is an anticorrelation at small

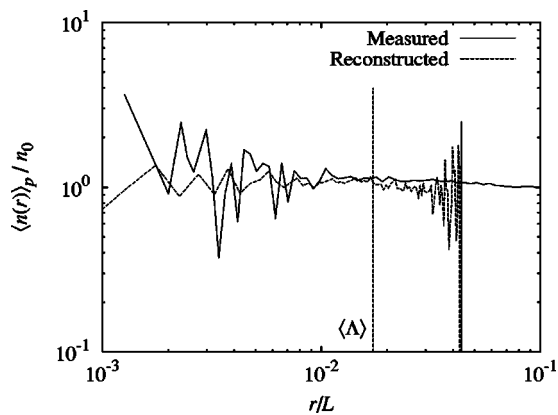


FIG. 13. Reconstruction of the conditional density from  $\omega(r)$  at  $t = 2\tau$  in the Poisson simulation with large softening simulation.

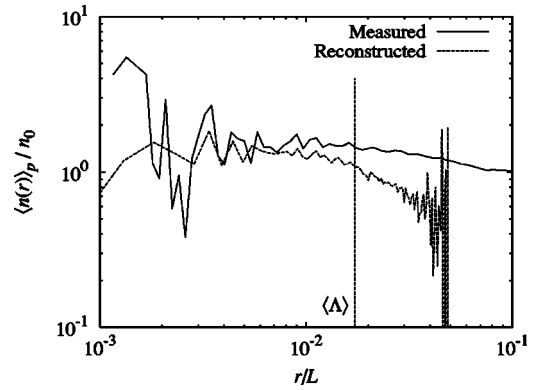


FIG. 14. Reconstruction of the conditional density from  $\omega(r)$  at  $t = 3\tau$  in the Poisson simulation with large softening simulation.

scales: the normalized conditional density is smaller than 1. This is due to the fact that two particles cannot be closer than a minimal distance which depends on  $a_s$ , the excluded volume feature being a typical property of *superhomogeneous* distributions [19]. This can be seen with the NN probability distribution, which is very peaked around the mean interparticle separation.

Figures 17–21 show the reconstructed conditional density (by using the NN probability distribution) and the one measured directly in the simulation. As for the Poisson case, one sees that the first structures observed via the conditional density are only due to a change of the NN probability distribution. Of course the dynamics of a particle with its NN are not described in the same way as for the Poisson case. The force on a particle cannot be approximated by the one from its NN, but the latter seems to be sufficiently important to give the direction of the particle displacement. Another interesting point is the fact that there are two phases in the clustering. This can be seen in Fig. 15: between  $t_0=0$  and  $t_1=\tau$  almost nothing happens, while between  $t_1=\tau$  and  $t_2=2\tau$  the correlations are quickly developed. As  $t_2-t_1=\tau$  is the typical time scale for two isolated particles, separated by a distance of order  $l$ , to fall on each other, this seems to show that this brutal change is a sign of such a behavior.

In order to verify this argument, we have done a simple test: we have run the simulation again but with a modified

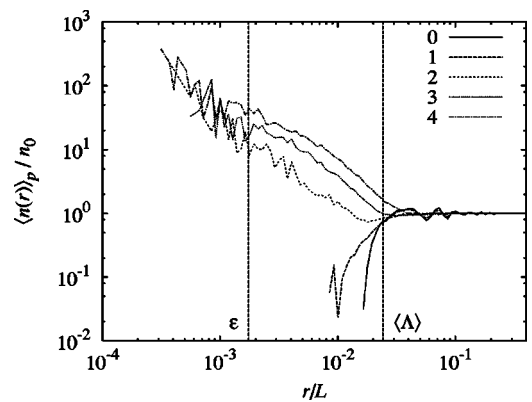


FIG. 15. Evolution of the normalized conditional density in the shuffled lattice distribution. The times are 0,1,2,3,4 in units of  $\tau$ .

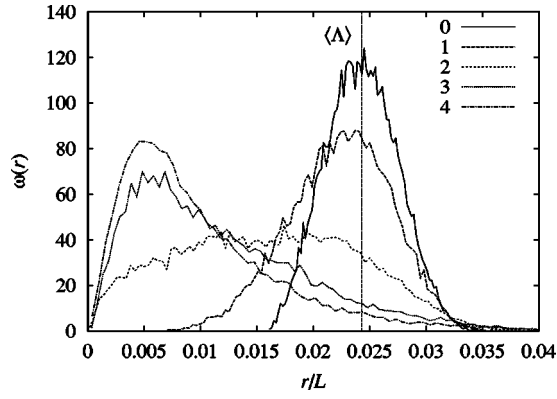


FIG. 16. Evolution of the NN probability distribution in the shuffled lattice for the same times as in Fig. 15.

integrator which, for a given particle, calculates the force acting on it only from its  $n$  NNs,  $n$  being an integer identical for all the particles, which can be chosen arbitrarily and changed during the simulation. For our study, we have done the following: (i) at  $t=0$ , the integrator finds the six NNs of each particle; (ii) it starts to evolve the system up to  $t=\tau$ , but at each time step the force on a particle is due only to the six particles, which were its six NNs at  $t=0$ ; (iii) at  $t=\tau$ , the integrator finds the NN neighbor of each particle; (iv) it continues the evolution up to  $t=2\tau$ , the force on a particle now being only the one from the particle which was its NN at  $t=\tau$ .

In Fig. 22, we show the result which confirms our assumption: between  $\tau$  and  $2\tau$ , the dynamics is driven by NN interaction. Furthermore, one can see that between 0 and  $\tau$ , what matters for a particle is the force from its six NNs chosen for the reason that in a perfect lattice, for a given particle, there is not a single NN but there are six NNs, all at the same distance  $\langle\Lambda\rangle$ . In the case of the lattice, these six particles are in a perfect symmetric configuration around the center particle (this is the case for all the particles when considered as centers). This implies that the force resulting from these particles cancels. In a shuffled lattice, as long as the parameter  $a_s$  is smaller than 1, this remains the case: even if there is a single NN for each particle, there are always five other particles which are almost at the same dis-

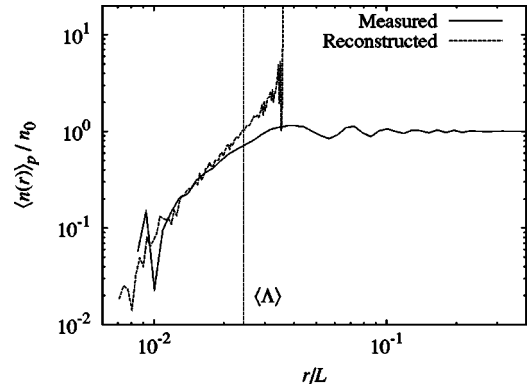


FIG. 18. Reconstruction of the conditional density from  $\omega(r)$  at  $t=\tau$  in the shuffled lattice.

tance as the NN. The simple test presented shows actually that the force from these six particles is what matters for the evolution of the correlations in the system between  $t=0$  and  $\tau$ , and the force from more distant particles is negligible.

Some simple calculations show actually that the force on a particle in a shuffled lattice is approximately given by

$$F_s = 2\sqrt{3} \frac{a_s}{l^2}, \quad (31)$$

assuming  $Gm^2=1$ . Looking at Fig. 23, one has, for instance, that the squared distance  $r_{01}$  between the central particle 0 and particle 1 is given by

$$r_{01}^2 = l^2 \left[ \left( 1 - \frac{\varepsilon_{1,x} - \varepsilon_{0,x}}{l} \right)^2 + \sum_{k=y,z} \left( \frac{\varepsilon_{1,k} - \varepsilon_{0,k}}{l} \right)^2 \right], \quad (32)$$

where  $\varepsilon_i = (\varepsilon_{i,x}, \varepsilon_{i,y}, \varepsilon_{i,z})$  is the displacement of the  $i$ th particle with respect to its lattice point. Supposing that these displacements are small compared to  $l$ , one finds that the force on the central particle from particle 1 is

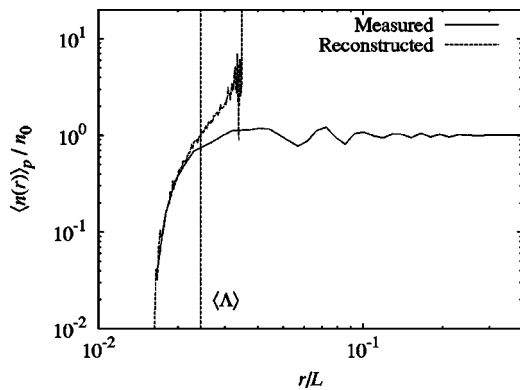


FIG. 17. Reconstruction of the conditional density from  $\omega(r)$  at  $t=0$  in the shuffled lattice.

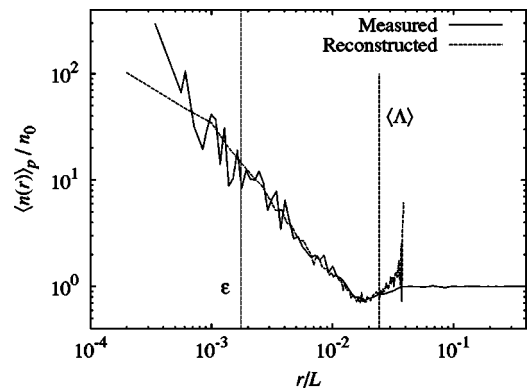


FIG. 19. Reconstruction of the conditional density from  $\omega(r)$  at  $t=2\tau$  in the shuffled lattice.

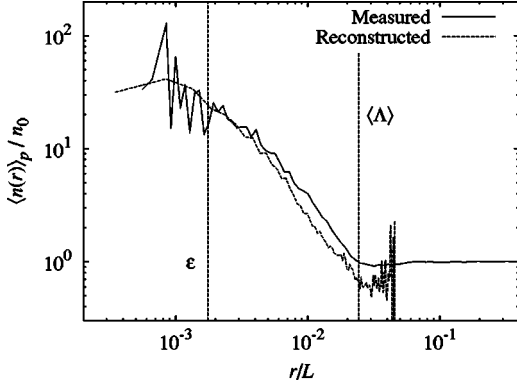


FIG. 20. Reconstruction of the conditional density from  $\omega(r)$  at  $t = 3\tau$  in the shuffled lattice.

$$F_{1,x} = \frac{2(\tilde{\varepsilon}_{0,x} - \tilde{\varepsilon}_{1,x}) - 1}{l^2} + O(\tilde{\varepsilon}^2), \quad (33a)$$

$$F_{1,k} = \frac{\tilde{\varepsilon}_{1,k} - \tilde{\varepsilon}_{0,k}}{l^2} + O(\tilde{\varepsilon}^2) \quad \text{for } k=y,z, \quad (33b)$$

with  $\tilde{\varepsilon}_{i,k} = \varepsilon_{i,k}/l$ . Making now the sum over the six particles around and averaging on all the  $\varepsilon_{i,k}$  which are random variables going from  $-\delta$  to  $\delta$ , one obtains  $\langle F_x \rangle = \langle \sum_1^6 F_{i,x} \rangle = 0$  and a variance  $\langle F_x^2 \rangle = 4\delta^2/l^6$ . This gives for the total squared force

$$\langle F^2 \rangle = \langle F_x^2 + F_y^2 + F_z^2 \rangle = \frac{12\delta^2}{l^6} \quad (34)$$

whose square root is given by Eq. (31). The force from the NN is given approximately by  $F_{NN} \approx l^{-2}$ , which shows that the real force is roughly

$$F_s \approx 2\sqrt{3}a_s F_{NN}. \quad (35)$$

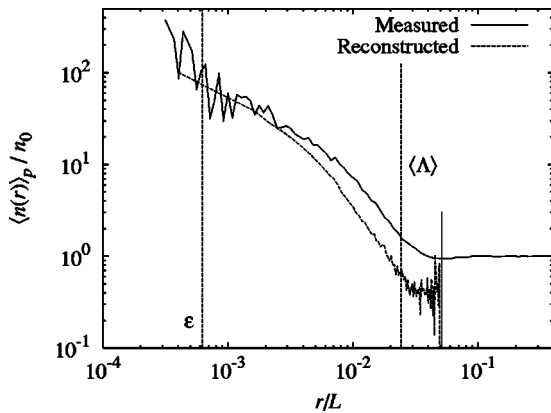


FIG. 21. Reconstruction of the conditional density from  $\omega(r)$  at  $t = 4\tau$  in the shuffled lattice.

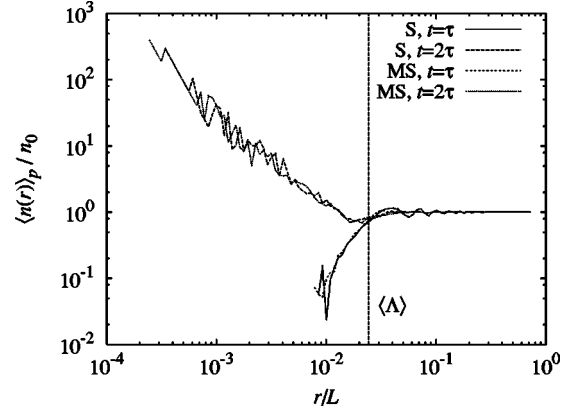


FIG. 22. Conditional density in the simulation (S) and in the modified simulation (MS) for the shuffled lattice.

One can estimate a time scale  $t_s$  defined by the relation  $l/2 = GmF_s t_s^2/2$  which is an approximative upper bound for the time scale needed by two NN particles to fall on each other,

$$t_s = \sqrt{\frac{2\pi}{\sqrt{3}a_s \sqrt{4\pi G\rho_0}}} \frac{1}{\sqrt{a_s}} \approx 1.7 \frac{\tau}{\sqrt{a_s}} \quad (36)$$

with  $\tau$  given by Eq. (15). Some simple numerical tests performed by varying  $a_s$  show that the real time scale is closer to

$$\tau_s \approx \frac{\tau}{\sqrt{a_s}} \lesssim t_s. \quad (37)$$

In our case, with  $a_s = 0.25$ , this gives  $\tau_s \approx 2\tau$  which is indeed in good agreement with the simulation.

In summary, while in a Poisson simulation, the correlations are made directly from the interaction between NN. In a shuffled lattice, there is a first phase in which a particle interacts mainly with its six NNs. This phase is characterized by strong anticorrelations which are slowly destroyed. This is then followed by a second phase in which some positive correlations are rapidly developed under some dynamics driven by NN interactions.

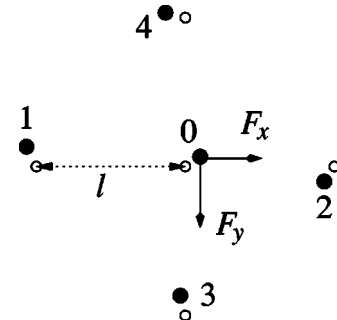


FIG. 23. Force in a shuffled lattice. The small circles (○) represent the lattice points while the black dots (●) represent the particles.

### B. CDM simulation

Finally, we study a CDM cosmological simulation which has been done by the Virgo Consortium [24]. This simulation is representative of many other cosmological simulations as their parameters, their initial particle configurations, and their small-scale properties are more or less always the same. The following discussion should therefore apply to other cosmological simulations of CDM type. Compared to the simulations we have done, this cosmological simulation is different on two points. First, there is space expansion. Secondly, the initial conditions (IC) are very elaborate. This last point needs some explanation.

The goal of this simulation is to study the evolution of a gravitating fluid made of CDM particles with particular initial correlations. As already mentioned, the particles in the simulation do not represent CDM particles but are a kind of cloud of CDM whose mass is of the order of a galaxy. This discretization of the fluid introduces some effects which are reduced by putting initially the particles in a particular way. The trick is to create first a distribution where the force on a particle is almost zero. In the Virgo case, this is done by running the integrator used for the simulation on a Poisson distribution with a negative gravity constant for a while. The distribution obtained is characterized by the fact that the main part of the force on a particle comes from large-scale mass fluctuations. The contribution from nearby particles is negligible. Note that the use of a repulsive gravity gives a behavior similar to a *one-component plasma* [9].

With this new distribution, it is necessary to apply a correlated displacement which would transform a continuous and perfectly uniform distribution into the expected CDM fluid, i.e., with a power spectrum on relatively large scales<sup>4</sup> behaving as  $P(k) \sim k^n$  with  $-3 < n < -1$ . This displacement field is applied by using the Zeldovich approximation, which also fixes the initial velocity of each particle as a function of its displacement. The distribution obtained is therefore correlated at all scales and has some small initial velocity.<sup>5</sup>

Note that as the preinitial distribution has superhomogeneous properties (as a lattice or a one-component plasma [19,9]) there are two main points to be considered: (i) on small scales the distribution continues to have the excluded volume feature typical of superhomogeneous systems, (ii) on large scales the correlation properties are given by a complex combination of the preinitial correlations (which are long-ranged) and by the correlations imposed by the displacement field. Whether the resulting fluctuation field has the same small-scale properties of the CDM continuous distribution is questionable [6–8,10]. However, here we are interested only in the small-scale features that have a clear imprint of the preinitial superhomogeneous distribution that is very similar, as we discuss below, to the shuffled lattice.

This simulation is made with  $N=256^3$  particles in a box of size  $L=239.5$  Mpc/h (where  $0.5 \leq h \leq 1$  is the dimension-

<sup>4</sup>It is not the aim of this simulation to consider the small  $k$  region where  $P(k) \sim k$ .

<sup>5</sup>Note that the velocities are small [6]. This is why afterwards we dare to compare this simulation with our initially static simulations.

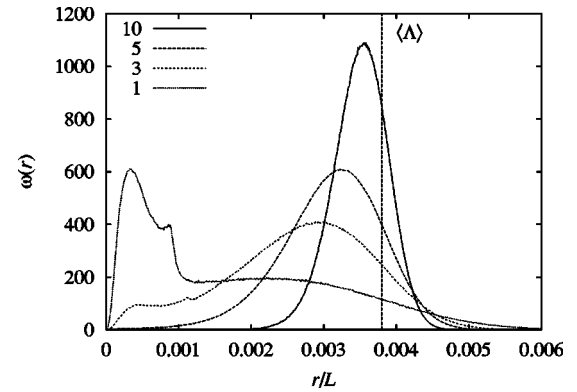


FIG. 24. Evolution of the NN probability distribution in the CDM simulation. The times are given by the redshift  $z$ .

less Hubble constant). The masses are such that  $\Omega = 1$  and it should represent a standard CDM model. The softening is  $\epsilon = 0.036$  Mpc/h, which gives  $\eta \approx 25$ . This simulation goes from a redshift  $z=50$  to  $z=0$ .

We have measured the conditional density and the NN probability distribution. With the latter we have used the approximation based on the NN probability distribution to compute the conditional density. The evolution of the NN probability distribution and the conditional density are shown in Figs. 24 and 25, while the results are shown in Figs. 26–28.

The first striking feature that we note is that the evolution is very similar to the shuffled lattice case. The conditional density, being initially that of an anticorrelated distribution, develops then positive power-law-like correlations at scales smaller than  $\langle \Lambda \rangle$ .

This evolution of the correlations is well described by using the NN probability distribution, which means that these correlations are simply due to correlations between NNs. In [15], we already analyzed this simulation. We observed that correlations started at the smallest scales of the system, i.e.,  $\epsilon < r < \langle \Lambda \rangle$ . Now with the relation between the NN probability distribution and the conditional density, we can make this observation more accurate: the “correlations at the smallest scales” are actually correlations between NNs. As in [15], we can again raise the question of whether these

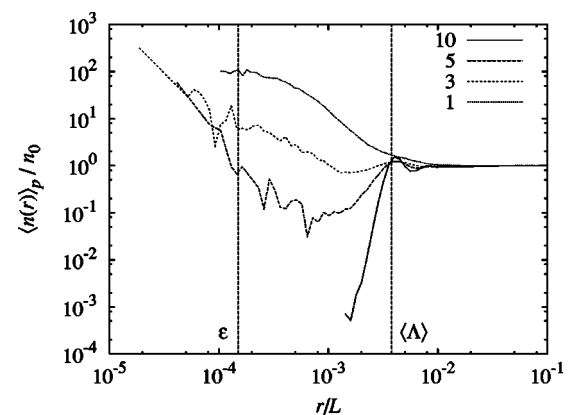


FIG. 25. Evolution of the conditional density in the CDM simulation. The times are given by the redshift  $z$ .

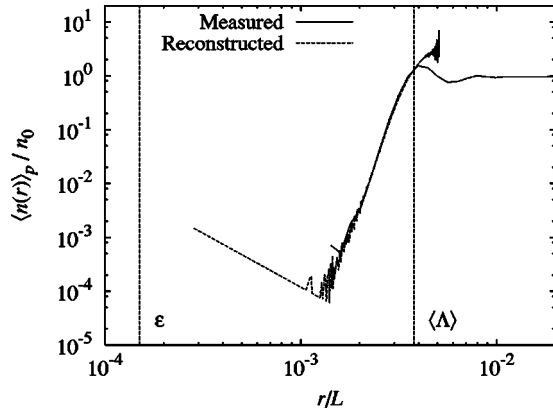


FIG. 26. Reconstruction of the conditional density from  $\omega(r)$  in the CDM simulation at  $z=10$ .

correlations are due to some interactions between NNs or are a “large-scale” effect, i.e., a consequence of the initial velocity field and the acceleration of the particles under the gravity of large-scale mass fluctuations. This large-scale effect is what we would expect from fluid dynamics.

The main point in [15] and [16] was the kind of universality of the correlations developed in different gravitating systems of particles, among them this CDM simulation, a Poisson simulation, and a shuffled lattice simulation. Now we can add that the first correlations are exactly of the same kind in all these simulations, namely NN correlations. In a Poisson and a shuffled lattice simulation, the discretization plays an important role in the creation of these correlations. This would suggest that it is the case for the CDM simulation.

## V. CONCLUSIONS

The fundamental relation used in this paper is Eq. (5). It relates the NN probability distribution  $\omega(r)$  to the conditional density  $\langle n(\mathbf{r}) \rangle_p$  at scales of the order of the average distance between NNs as long as most of the particles have a clear NN. By checking if this relation holds in a simulation,

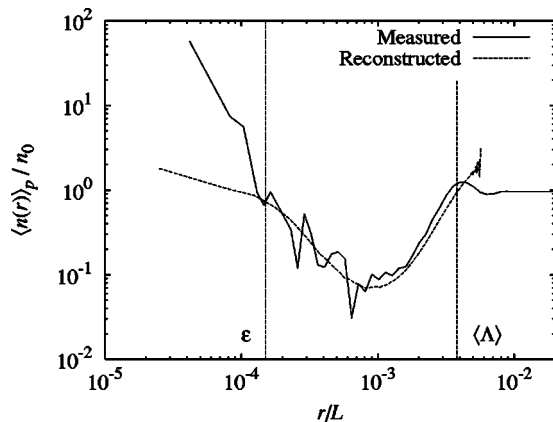


FIG. 27. Reconstruction of the conditional density from  $\omega(r)$  in the CDM simulation at  $z=5$ . Note that the discrepancy at scales below  $\epsilon$  comes from a too small statistics on the measured conditional density.

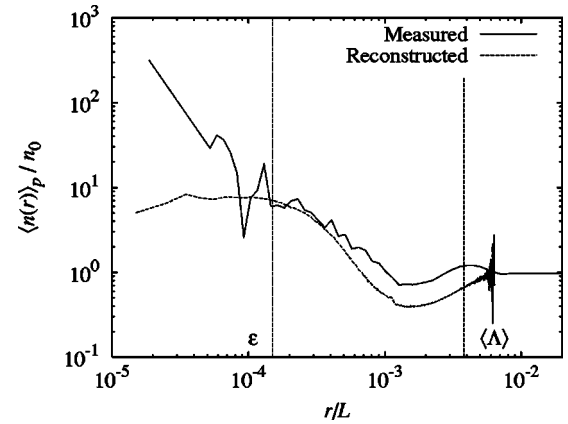


FIG. 28. Reconstruction of the conditional density from  $\omega(r)$  in the CDM simulation at  $z=3$ . Note that the discrepancy at scales below  $\epsilon$  comes from a too small statistics on the measured conditional density.

we get an interesting piece of information on the nature of the correlations: are they only due to NN correlations or do they show the existence of structures made of many particles?

In the three simulations that we have considered, Poisson, shuffled lattice, and CDM, which are high-resolution ones ( $\eta \gg 1$ ), we have seen that this relation holds at early times showing that the correlations grow by being initially only NN correlations. In another simulation, Poisson with large softening such that  $\eta \ll 1$ , we have seen that this is not the case anymore. In this simulation, the first correlations are due directly to the formations of large structures—i.e., larger than the typical distance between NNs—containing more than two particles.

The results for the high-resolution Poisson simulation and for the shuffled lattice have encouraged us to push the analysis a bit further. In the Poisson case, using the relation (5) and considering that (i) the force on a particle is mainly due to its NN and (ii) for more than half of the particles, two particles are mutually NN, we could treat the system as a set of isolated two-body systems. Knowing the initial NN probability distribution and using the Liouville theorem, it was then possible to find the early evolution of the correlations with quite a lot of precision.

In the shuffled lattice simulation, we have observed that at the beginning the situation was more complex than in the Poisson case. Due to the approximative symmetries, the early evolution involves interactions between more than two particles. Actually, in this case, instead of having a single NN for each particle, there are six particles which lie at almost the same distance: such a situation changes the small-scale behavior of the force on an average particle by introducing a compensation, which is exact and gives a null force only when the lattice case is considered. However, the result is similar to the Poisson case: the formation of correlations between NNs. At a later time, the situation becomes exactly identical to the Poisson case as the system behaves like a set of isolated two-body systems. The consequence is a rapid growth of the correlations between NNs.

For the CDM simulation, we have not tested whether the

evolution could be explained at a certain time by NN interactions. This is a really important question because this simulation is supposed to describe a fluid. The particles are not meant to describe particles but mass tracers: they should follow the flow due to gravity from the large-scale mass fluctuations. If this simulation had the same dynamics as the Poisson and shuffled lattice simulations, that is, if it could be explained by NN interactions in a small amount of time, this would clearly show that the fluid is not well simulated, as the evolution would be influenced by the discrete nature of these particles resulting from the discretization of the fluid and thus it would not exist in a real fluid. This would then require some careful study in order to understand how these effects influence the later evolution.

In some previous papers [15,16] we already raised these questions, after having observed the kind of universal correlations developed in different simulations all characterized by their particle-based dynamics. In some recent papers [13,14], others authors have also analyzed the influence that these particles could have on the evolution, but only as a consequence of close encounters between these particles. Their conclusions were that the particles have an influence on the density profile of the clusters.

In this paper, we have tried to bring a new element to the understanding of what happens in several high-resolution simulations, including the cosmological CDM one, by showing the nature of the first correlations developed. We also raise some new questions which clearly deserve further study. From our results, we now argue for three conclusions about the nature of clustering in the nonlinear regime observed in these NBS. With respect to cosmological NBS, we conclude that the exponent characterizing the nonlinear clustering observed has essentially nothing to do with (i) the expansion of the Universe or (ii) the nature of the small initial fluctuations imposed in the IC. We further present evidence for a qualitative description of the dynamics driving this clustering given in [11] based on the Poisson case, and in [15] based on a similar analysis of the CDM simulation. (iii) The nonlinear clustering develops from the large fluctuations intrinsic to the particle distribution at small scales (specifically around the smallest resolved scale  $\epsilon$ ). In particular, we show here that the exponent characterizing it can be seen to

emerge at early times in the simulations when the evolution is well approximated as being due only to the interactions between NN particles.

A more quantitative description of this dynamics is evidently needed, with the principal goal being to understand the specific value of the exponent. In the cosmological literature (see, e.g., [1]), the idea is widely dispersed that the exponents in nonlinear clustering are related to that of the initial power spectrum of the small fluctuations in the CDM fluid, and even that the nonlinear two-point correlation can be considered an analytic function of the initial two-point correlations [25,26] (although see [2], where more emphasis is put on the tendency for IC to be washed out in the nonlinear regime). The models used to explain the behavior in the nonlinear regime usually involve both the expansion of the Universe and a description of the clustering in terms of the evolution of a continuous fluid. We have argued that the exponent is universal in a very wide sense, being common to the nonlinear clustering observed in the nonexpanding case. It would appear that the framework for understanding the nonlinear clustering must be one in which discreteness (and hence intrinsically nonanalytical behavior of the density field) is central, and that the simple context of nonexpanding models should be sufficient to elucidate the essential physics. Note that we have not discussed here the *amplitude* of the correlation function, and in particular how it evolves in time, which is directly related to the time evolution of the scale of nonlinearity. This is where the fluctuations at large scales, which are different in the various IC considered, can play a role as envisaged in the cosmological context (through the linear amplification of power at large scales). We will address this question further, again considering nonexpanding models, in future work.

#### ACKNOWLEDGMENTS

We warmly thank D. Pfenniger at the Observatory of Geneva for the use of the GRAVITOR cluster to run numerical simulations. We thank M. Joyce, A. Gabrielli, L. Pietronero, A. Melott, and R. Durrer for very useful discussions and comments. F.S.L. acknowledges the support of the Marie Curie Fund through Grant No. HPMF-CT-2001-01443 and the University of Geneva for the kind hospitality.

- 
- [1] P. J. E. Peebles, *The Large-Scale Structure of the Universe* (Princeton University Press, Princeton, NJ, 1980).
  - [2] W. C. Saslaw, *The Distribution of the Galaxies* (Cambridge University Press, Cambridge, UK, 2000).
  - [3] A. Melott, *Comments. Astrophys. J.* **15**, 1 (1990).
  - [4] B. Kuhlman, A. Melott, and S.F. Shandarin, *Astrophys. J. Lett.* **470**, L41 (1996).
  - [5] R.J. Splinter, A.L. Melott, S. Shandarin, and Y. Suto, *Astrophys. J.* **497**, 38 (1998).
  - [6] T. Baertschiger and F. Sylos Labini, *Europhys. Lett.* **57**, 322 (2002).
  - [7] T. Baertschiger and F. Sylos Labini, *Europhys. Lett.* **63**, 633 (2003).
  - [8] A. Dominguez and A. Knebe, *Europhys. Lett.* **63**, 631 (2003).
  - [9] A. Gabrielli, B. Jancovici, M. Joyce, J. Lebowitz, L. Pietronero, and F. Sylos Labini, *Phys. Rev. D* **67**, 043506 (2003).
  - [10] A. Gabrielli, in preparation.
  - [11] M. Bottaccio, R. Capuzzo-Dolcetta, P. Mionchi, M. Montuori, and L. Pietronero, *Europhys. Lett.* **7**, 315 (2002).
  - [12] R. Mohayaee and L. Pietronero, *Physica A* **323**, 445 (2003).
  - [13] J. Diamond, B. Moore, J. Stadel, and S. Kazantzidis, *Mon. Not. R. Astron. Soc.* **348**, 977 (2004).
  - [14] J. Binney and A. Knebe, *Mon. Not. R. Astron. Soc.* **333**, 378 (2002).
  - [15] T. Baertschiger, M. Joyce, and F. Sylos Labini, *Astrophys. J. Lett.* **581**, L63 (2002).
  - [16] F. Sylos Labini, T. Baertschiger, and M. Joyce, *Europhys. Lett.* **66**, 171 (2004).

- [17] M. Bottaccio, L. Pietronero, A. Amici, P. Miocchi, R. Capuzzo Dolcetta, and M. Montuori, *Physica A* **305**, 247 (2002).
- [18] S. Chandrasekhar, *Rev. Mod. Phys.* **15**, 1 (1943).
- [19] A. Gabrielli, M. Joyce, and F. Sylos Labini, *Phys. Rev. D* **65**, 083523 (2002).
- [20] J.R. Dorfman, *An Introduction to Chaos in Nonequilibrium Statistical Mechanics* (Cambridge University Press, Cambridge, UK, 2001).
- [21] G. Gallavotti, *The Elements of Mechanics* (Springer-Verlag, Berlin, 1983).
- [22] <http://www.mpa-garching.mpg.de/gadget/>.
- [23] J. Binney and S. Tremaine, *Galactic Dynamics* (Princeton University Press, Princeton, NJ, 1987).
- [24] A. Jenkins, C.S. Frenk, F.R. Pearce, P.A. Thomas, J.M. Colberg, S.D.M. White, H.M.P. Couchman, J.A. Peacock, G. Efsthathiou, and A.H. Nelson, *Astrophys. J.* **499**, 20 (1998).
- [25] A.J.S. Hamilton, P. Kumar, E. Lu, and A. Matthews, *Astrophys. J. Lett.* **374**, L1 (1991).
- [26] J. Peacock and S. Dodds, *Mon. Not. R. Astron. Soc.* **280**, L19 (1996).